Proc. 14th INA Conf., Reston VA, USA (Guest Ed. J. Self-Trail)
J. Nannoplankton Res. **35** (2), 2015, pp.129-139

ISSN 1210-8049 Printed by The Sheridan Press, USA

Global decline in the calcareous nannofossil productivity indicator *Biscutum* in the Cretaceous

Bobbi Brace*, David Watkins

214 Bessey Hall, Department of Earth and Atmospheric Sciences, University of Nebraska-Lincoln, Lincoln, Nebraska 68588, USA; *bobbibrace@huskers.unl.edu

Manuscript received 27th March, 2015; revised manuscript accepted 25th June, 2015

Abstract The relative abundance of *Biscutum* in calcareous nannofossil assemblages is commonly used as a proxy for surface-water fertility. This utility as an indicator of elevated fertility in surface waters has led to the use of *Biscutum* abundances in investigations of oceanic anoxic events, which are often associated with elevated surface-water productivity. This study presents a global dataset of *Biscutum* relative-abundance values through the Cretaceous. Previously unpublished abundance data from a composite section of North American mid-latitude localities are also included. After an Albian/Cenomanian (nannofossil zones CC8-10) peak, an abrupt global decrease in the relative abundance of *Biscutum* occurred in the Turonian (CC11). After this decrease, average relative abundance values never again approached pre-Turonian levels. The average relative abundance after the decrease was less than half of the pre-Turonian average. The onset of extreme palaeoceanographic conditions associated with Oceanic Anoxic Event 2 may have permanently disrupted the role of *Biscutum* as the primary productivity indicator for the remainder of the Cretaceous, however, the unidirectional nature of the abundance shift suggests that a more permanent driver affected *Biscutum*. This permanent change may be linked to initiation of widespread chalk deposition by the Late Albian, a stabilised mode of ocean circulation, increased water-column stratification and nutrient partitioning between surface and deeper waters, thereby altering the evolution of *Biscutum* for the rest of the Cretaceous.

Keywords *Biscutum*, Late Cretaceous, palaeoproductivity, oceanic anoxic event, evolution

1. Introduction

Elevated abundances of *Biscutum*, in association with high surface-water fertility conditions, have been reported in several quantitative studies from a variety of settings. *Biscutum* is widely recognised as one of the most extreme Cretaceous examples of *r*-selected (opportunist) taxa that were adapted to eutrophic environments (Bown, 2005). Roth (1981) was the first to use *Biscutum constans* as an indicator of high-fertility surface-water conditions, by associating former upwelling sites with high species abundances. Roth & Bowdler (1981) noted the prevalence of *B. constans* and *B. gartneri* in neritic assemblages purported to be associated with advection of nutrient-rich waters. Roth & Krumbach (1986) later used statistical analyses to demonstrate the relationship between *B. constans*, *Zeugrhabdotus* (as *Zygodiscus*) *erectus*, and high surface-water fertility conditions. Watkins' (1989) study of cyclically-bedded shales and chalks in the Western Interior Basin of North America demonstrated that significantly higher abundances of *B. constans* occured in low-diversity marl deposits, suggesting that the marls were deposited during times of relatively high productivity (*i.e.* mesotrophy), dominated by the fertility indicators *B. constans* and *Z. erectus*. Later studies agreed with Watkins' (1989) conclusions and additionally suggested that *B. constans* may be associated with mesotrophic, rather than eutrophic, surface-water conditions, based on variable distributions of *B. constans* and *Zeugrhabdotus* sp. (Erba, 1992; Erba *et al*., 1992).

The utility of *Biscutum* as a surface-water fertility proxy has led to its use in the study of oceanic anoxic events (OAEs: *e.g.* Erba, 2004; Bornemann *et al*., 2005; Eleson & Bralower, 2005; Watkins *et al*., 2005; Linnert *et al*., 2010, 2011), which, in some cases, may have been caused by increased surface-water productivity. Short-term changes associated with OAEs (*e.g.* isotopic shifts, species abundance fluctuations) were superimposed onto long-term, fundamental shifts, which occurred during the Cretaceous, including changes in ocean circulation, water-column structure, nutrient partitioning, pelagic sedimentation, sea level and climate (*e.g.* Leckie *et al*., 2002; Hay, 2008; Giorgioni *et al*., 2015). Significant changes also occurred within marine plankton communities. During the great mid-Cretaceous transgression, calcareous plankton invaded epeiric seas and found new ecospace for proliferation. As such, Late Cretaceous nannoplankton communities were distinct from those of the Early Cretaceous, due to the appearance and radiation of several new coccolith and nannolith groups (*e.g. Prediscosphaera*, *Micula*, *Quadrum*, *Lithastrinus*, *Kamptnerius*, *Ceratolithoides*, *Cal-*

culites, Aspidolithus and *Lucianorhabdus*: Bown *et al*., 2004; Erba, 2006).

Perhaps the most striking difference between Upper and Lower Cretaceous strata is the shift from predominately black shale to chalk deposition during the middle Cretaceous (Hay, 1995: Giorgioni *et al*., 2015). The origin of Cretaceous chalk remains controversial, and several factors likely contributed to the observed shift in global sedimentation patterns. As levels of volcanism and ocean-crust production increased in the Early Cretaceous, sea level rose and Earth warmed appreciably. Increased hydrothermal activity, due to increased rates of sea-floor spreading, and reduced oceanic Mg/Ca ratios may have preconditioned the ocean for the spread of pelagic carbonate (Stanley & Hardie, 1998). Continental margins were flooded, resulting in the formation of shallow, epeiric seas (Hay, 2008). The creation of warm, stratified seas during the Albian through Turonian resulted in a shift in the ecosystem structure of marine plankton communities, as waters in the euphotic zone became nutrient-starved (Leckie *et al*., 2002). Homogeneous $\delta^{13}C$ values in the Upper Albian signal a change toward a more stable ocean-circulation mode, as compared to earlier times (Giorgioni *et al*., 2015). Ocean basins became more connected, while the thermocline, surface currents and bottom-water ventilation stabilised (Giorgioni *et al*., 2015). Deposition shifted from primarily organic-carbon-rich black shales in Tethyan basins to chalk deposition along flooded continental margins and, eventually, in open-ocean settings (Leckie *et al*., 2002; Giorgioni *et al*., 2015). All of the above processes combined to result in stratified, oligotrophic to mesotrophic, carbonate-based ecosystems, which came to characterise the chalk seas for the remainder of the Late Cretaceous.

A global synthesis of Valanginian to Maastrichtian *Biscutum* relative abundance data is presented, as compiled from 19 published datasets, as well as a new dataset from North America. The incorporated sections cover a wide range of geographic and oceanographic settings, and the resulting compilation is evaluated in light of Cretaceous palaeoceanography.

2. Materials and methods

Abundance data presented in this study were collected from 19 published datasets, the majority of which were generated in conjunction with the Deep Sea Drilling Program (DSDP) or Ocean Drilling Program (ODP; Figure 1, Table 1). The selected datasets were chosen with the aim of providing a globally-representative set of *Biscutum* abundance data that encompasses a range of latitudes and oceanographic settings. Of the 19 datasets, 16 contain semi-quantitative *Biscutum* abundance data, while three include quantitative data (Table 1). In order to provide a common temporal framework, all samples were assigned to a CC nannofossil zone (after Perch-Nielsen, 1985). Inability to assign samples to a zone generally resulted from a paucity of marker-species used in the CC zonation scheme. Samples with poor preservation were excluded from analysis in order to avoid preservational bias in the abundance data. The sample preparation methodology used in the published studies is consistent, with only minor differences. With the exception of two studies, all of the previously-published data were collected from samples prepared using simple smear-slide techniques; Cepek (1978) and Cepek (1981) prepared smear-slides from sediment samples pre-treated with an ultrasonic apparatus. Since the preparation methods are similar across studies, we did not anticipate any bias in the physical distribution of the coccoliths, and thus bias resulting from varying methodologies in the resulting datasets.

In order to facilitate comparison, relative abundance data from each sample were standardised. The relative abundance categories used by the majority of authors included in the database were selected as the standard categories (Table 1). Data requiring normalisation was minimised by choosing the categories used by most authors to serve as that standard. Data classified using an alternative scheme were normalised to fit the standardised categories. For example, Ladner & Wise (1989) determined a taxon to be 'rare' if one specimen was documented in 101-1000 fields of view (FOV) and 'few' if one specimen was observed per 11-100 FOV. In the standardised categories adopted here, taxa that the authors classified as 'rare' or 'few' are considered 'rare' (*i.e*. one specimen per 11-≥200 FOV) in the standardised categories. Standardised relative abundance categories were also applied to quantitative data, as shown in Table 2.

All data were normalised per zone, in order to avoid sampling bias. Some events or intervals in the Cretaceous, such as OAEs, are more frequently investigated than others. In order to avoid bias due to the inequal distribution of studied sections in the Cretaceous, relative abundance

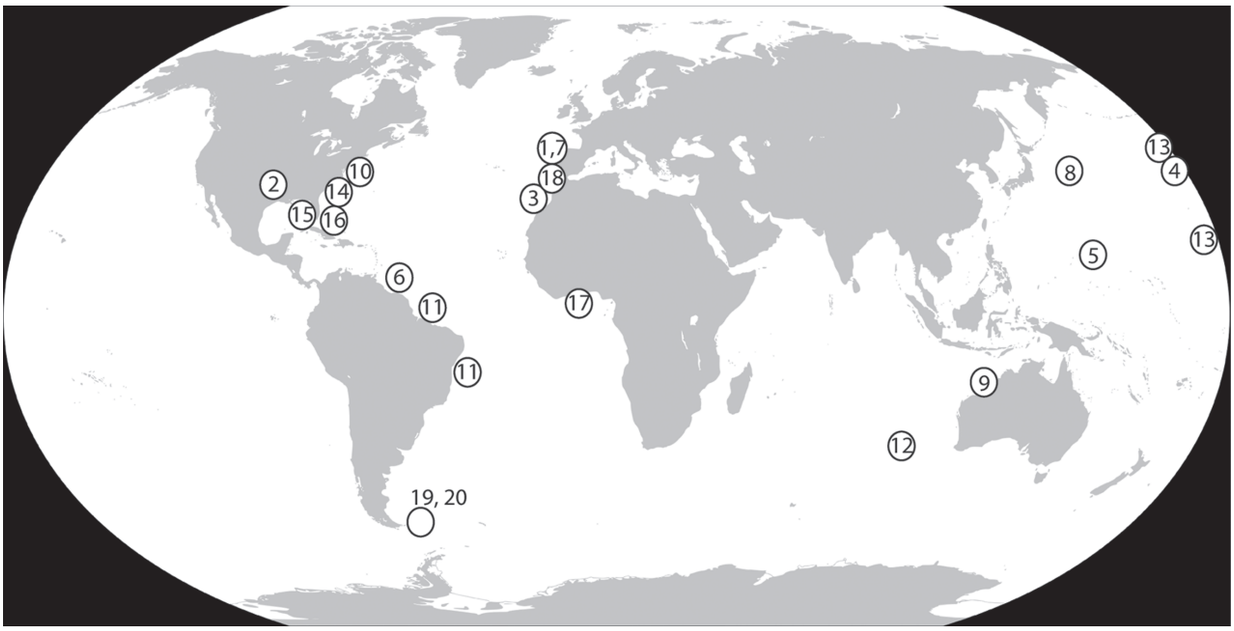

Figure 1: Location of datasets (see Table 1 for author information)

Location	Study Age Range	Citation
North Atlantic Ocean	Aptian-Cenomanian	(1) Applegate & Bergen, 1988
North Atlantic Ocean	Albian-Coniacian	(3) Cepek, 1978
North Atlantic Ocean	Campanian-Maastrichtian	(7) Ladner & Wise, 2001
North Atlantic Ocean	Albian-Maastrichtian	(10) Okada & Thierstein, 1979
North Atlantic Ocean	Campanian-Maastrichtian	(14) Schmidt, 1978
North Atlantic Ocean	Albian-Cenomanian	(18) Wiegand, 1984
Atlantic Ocean	Albian	(6) Kulhanek & Wise, 2006
Atlantic Ocean	Albian-Maastrichtian	(16) Watkins & Verbeek, 1988
Atlantic Ocean	Albian-Santonian	(17) Watkins *et al*., 1998
Atlantic Ocean	Aptian-Campanian	(19) Wise, 1983
Atlantic Ocean	Aptian-Maastrichtian	(20) Wise & Wind, 1977
South Atlantic Ocean	Albian-Maastrichtian	(11) Perch-Nielsen, 1977
North America	Albian-Maastrichtian	(2) Brace & Watkins, 2014*
Gulf of Mexico	Berriasian-Cenomanian	(15) Watkins & Bowdler, 1984
North Pacific Ocean	Aptian-Maastrichtian	(4) Cepek, 1981
Pacific Ocean	Aptian-Cenomanian	(5) Erba, 1992*
Pacific Ocean	Berriasian-Maastrichtian	(8) Lees & Bown, 2005
Pacific Ocean	Aptian-Turonian	(13) Roth, 1981*
Indian Ocean	Aptian-Maastrichtian	(9) Moran, 1992
Indian Ocean	Turonian-Maastrichtian	(12) Resiwati, 1991

Table 1: Locations, age ranges and references of datasets. *Quantitative relative abundance data (all other references contain semi-quantitative data)

Relative abundance category	Semi-quantitative criteria	Fully-quantitative criteria (% of total assemblage)
X (Absent)	no occurrences	no occurrences
R (Rare)	1 specimen per 11->200 FOV	<2%
F (Few)	1 specimen per 2-10 FOV	2-10%
C (Common)	1-10 specimens per FOV	11-20%
A (Abundant)	>10 specimens per FOV	21-40%
D (Dominant)	>100 specimens per FOV	>40%

Table 2: Standardised relative abundance categories applied to composite dataset

datapoints were normalised per CC zone. This was accomplished by dividing the total number of datapoints in each zone by the number of occurrences in a given relative abundance category. For example, 67 of the 885 total datapoints fall within CC10. Of those 67 samples, 46.3% (31/67 samples) were classified as 'common'. This point is plotted in CC10 corresponding to the 'common' relative abundance category. The size of the point is proportional to the number of 'common' occurrences out of total occurrences in CC10. Assigning samples to common biostratigraphic zones and relative abundance categories, and normalising by zone, eliminates sampling bias, facilitates comparison across different types of data, and presents the data clearly to allow investigation of abundance trends through time.

Previously-unpublished abundance data are included from 147 samples from five North American localities: three from the Western

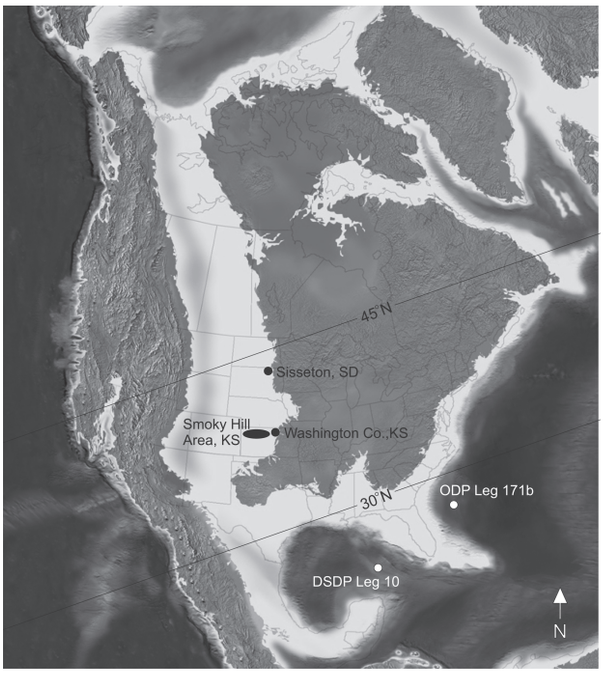

Figure 2: Late Cretaceous palaeogeographic reconstruction of North America (modified from Blakey, 2012; palaeolatitudes estimated), showing localities used to generate new relative abundance dataset

Interior Basin (Washington County, Kansas; Smoky Hill type-area; Sisseton, North Dakota), one from the North Atlantic Ocean (ODP Leg 171B, Holes 1049A, 1050C and 1052E) and one from the Gulf of Mexico (DSDP Leg 10, Site 95: Figure 2). Sample locations were chosen based on average preservation and stratigraphic coverage, as previously established by Shamrock & Watkins (2009). Samples with low nannofossil abundance and/or poor preservation were excluded. All samples from which new data are presented were prepared using the slurry-smear method (Watkins & Bergen, 2003) and examined using an Olympus BX-51 light microscope at 1250x magnification. Relative abundance data are included only for the *Biscutum constans/ellipticum*-type species (*i.e. Biscutum ubiquem* of Brace & Watkins, 2014). Other species of *Biscutum* (*e.g. B. coronum, B. dissimilis, B. melaniae, B. notaculum*) are not included in the analyses, as they do not comprise a significant portion of the overall assemblage and have no known utility as productivity indicators.

3. Results

A total of 885 samples were included in this study, after excluding those that were not constrained to a CC zone or were poorly preserved. Quantitative data were collected from 212 of the 885 total samples, while the remaining 673 consist of semi-quantitative data. All of the data are presented together in Figure 3, while Figure 4 shows only the quantitative data subset.

Figure 3 presents the total compilation of standardised *Biscutum* relative-abundance data. Each sample was assigned to a CC zone and placed in one of six abundance categories, according to the standardised relative abundance categories described in Table 1. The relative abundance of *Biscutum* species is 'common' from the Valanginian through the Lower Turonian (CC7 to CC11), barren through the Middle Turonian and Coniacian (CC12 to CC15), and 'rare' and 'few' through the rest of the Upper Cretaceous (Santonian through Maastrichtian, CC16 to CC26).

Figure 4 contains the quantitative subset of *Biscutum* relative-abundance data. No abundance standardisation was applied; the data are plotted directly without normalisation. Again, each sample was assigned to a CC zone. Each point on the graph in Figure 4 is equal to one datapoint. Of the 885 total samples, 212 contain quantitative abundance data and are included in Figure 4 (see Table 1 for citations). Peak relative abundance of *Biscutum* species from CC8 to CC10 (Albian to Upper Cenomanian) exceeds 35%. Beginning in the Lower Turonian (CC11), abundances rapidly declined and never again achieve similarly high levels. This same pattern of decreasing abundance near the Cenomanian/Turonian boundary, and permanently decreased abundances beyond that, reflected in the quantitative data subset (Figure 4) are also apparent in the semi-quantitative data (Figure 3).

Upon examination of Figures 3 and 4, it is clear that a considerable and unidirectional decrease in the relative abundance of *Biscutum* species began in CC11 (Lower Turonian). Prior to CC11, maximum relative abundances of *Biscutum* ranged from 13% to 41.4%, with an average value of 18.7%. From CC11 through CC26 (Lower Turonian through Maastrichtian), the maximum relative abundances decreased and the average relative abundance of *Biscutum* dropped precipitously to 8.8%. This is less than half of the pre-CC11 average. The relative abundance values from CC7 through CC11 are statistically different from the abundances documented in CC13 through CC26, as shown by a post hoc Tukey test (p=8.6x10^{-6}).

The only exceptions to the observed trend of decreasing abundance from CC11 (Lower Turonian) through the

end of the Cretaceous are three outliers in CC23 and CC24, as indicated in Figure 4. These three datapoints come from the new North American dataset. Two of the datapoints are from Hole 1049A at Blake Nose (25.0 and 26.1%), while the third is from Sisseton, SD (22.9%). Blake Nose is located on the North American continental shelf, while the Sisseton locality was located in an interior seaway. The cause of the high relative abundances is unclear, but the apparent spike in relative abundances against otherwise-low background values at two oceanographically distinct sites suggests that the results are not artifacts, but are representative of widespread conditions at that time, although determination of the exact nature of these outliers requires further investigation.

4. Discussion

Biscutum abundance values in the Late Cretaceous never again achieved levels attained prior to CC11 (Early Turonian; Figures 3, 4). Figure 3 shows the majority of occurrences per zone prior to the mid-Cretaceous as falling within the 'common' relative abundance category. After the abundance shift in CC11, most datapoints fall within the 'few' and 'rare' categories; 'common' occurrences after CC11 consist of <15% of the datapoints per zone. It is important to note that, although the shift in relative abundance from 'common' to 'few' may appear nominal, the semi-quantitative abundance categories differ from one another by approximately one order of magnitude (Table 2). The inflection point of the observed decrease in the mid-Cretaceous (CC11) corresponds with the onset of fundamental changes in the Cretaceous ocean-climate system, including widespread deposition of chalk, associated with nutrient partitioning between surface and deeper waters, and a more stable mode of ocean circulation (Leckie *et al*., 2002; Giorgioni *et al*., 2015).

As levels of volcanism and ocean-crust production increased, starting in the Early Cretaceous, sea-level rose and Earth warmed appreciably. Continental margins were flooded, resulting in the formation of shallow, epeiric seaways (*e.g*. Hay, 2008). The creation of warm, stratified seas during the Albian through Turonian resulted in a shift in the ecosystem structure of marine plankton communities, as waters in the euphotic zone became nutrient-starved. Deposition shifted from primarily organic-carbon-rich black shales in Tethyan basins to chalk deposition along flooded continental margins (*e.g*. Leckie *et al*., 2002). All of the above processes combined to result in stratified, oligotrophic to mesotrophic, carbonate-based ecosystems, which came to characterise the chalk seas for the remainder of the Late Cretaceous.

Several authors have used the opportunist *Biscutum* to identify occurrences of elevated surface-water productivity (*e.g*. Roth, 1981; Roth & Bowdler, 1981; Roth & Krumbach, 1986; Watkins, 1989; Erba, 1992; Erba *et al*., 1992; Erba, 2004; Bornemann *et al*., 2005; Eleson & Bralower, 2005; Watkins *et al*., 2005; Linnert *et al*., 2010, 2011). In Watkins' (1989) study of the Western Interior Seaway, he noted increased abundances of *Biscutum constans* and low nannofossil diversity in marls associated with mesotrophic surface-water conditions. Similarly, Lower Cretaceous strata dominated by black shale deposition are shown in the current study to have much higher abundances of *Biscutum* than the Upper Cretaceous strata dominated by chalk deposition. The decrease in *Biscutum* relative abundance values occurs in the mid-Cretaceous, coincident with the onset of chalk deposition and associated nutrient partitioning.

As widespread chalk deposition was initiated, the mesotrophic to eutrophic *Biscutum* may have been negatively impacted by concomitant reduction of nutrients in the surface water. As demonstrated in several previous studies, *Biscutum* comprises a significant portion of nannofossil assemblages during periods of elevated surface-water fertility until the middle Cretaceous. With the onset of upper water-column stratification and nutrient partitioning, areas of elevated nutrients were limited and, as such, areas where the opportunist *Biscutum* could proliferate were limited as well.

This large-scale, fundamental ocean-climate-system transition was punctuated at the Cenomanian-Turonian boundary by OAE2, one of the largest global-carbon-cycle perturbations of the Phanerozoic (*e.g*. van Helmond *et al*., 2013). OAE2 is associated with burial of massive amounts of organic carbon, which resulted in a >2‰ positive carbon isotope excursion (Arthur *et al*., 1988) and peak global temperatures (*e.g*. Wilson *et al*., 2002; Forster *et al*., 2007), related to high levels of atmospheric CO_2. Volcanism, specifically emplacement of the Caribbean Plateau, is considered a possible triggering mechanism for the extreme warmth, as well as a source of biolimiting trace metals (Erba, 2004). Recent work also suggests that the OAE2 interval was characterised by an accelerated hy-

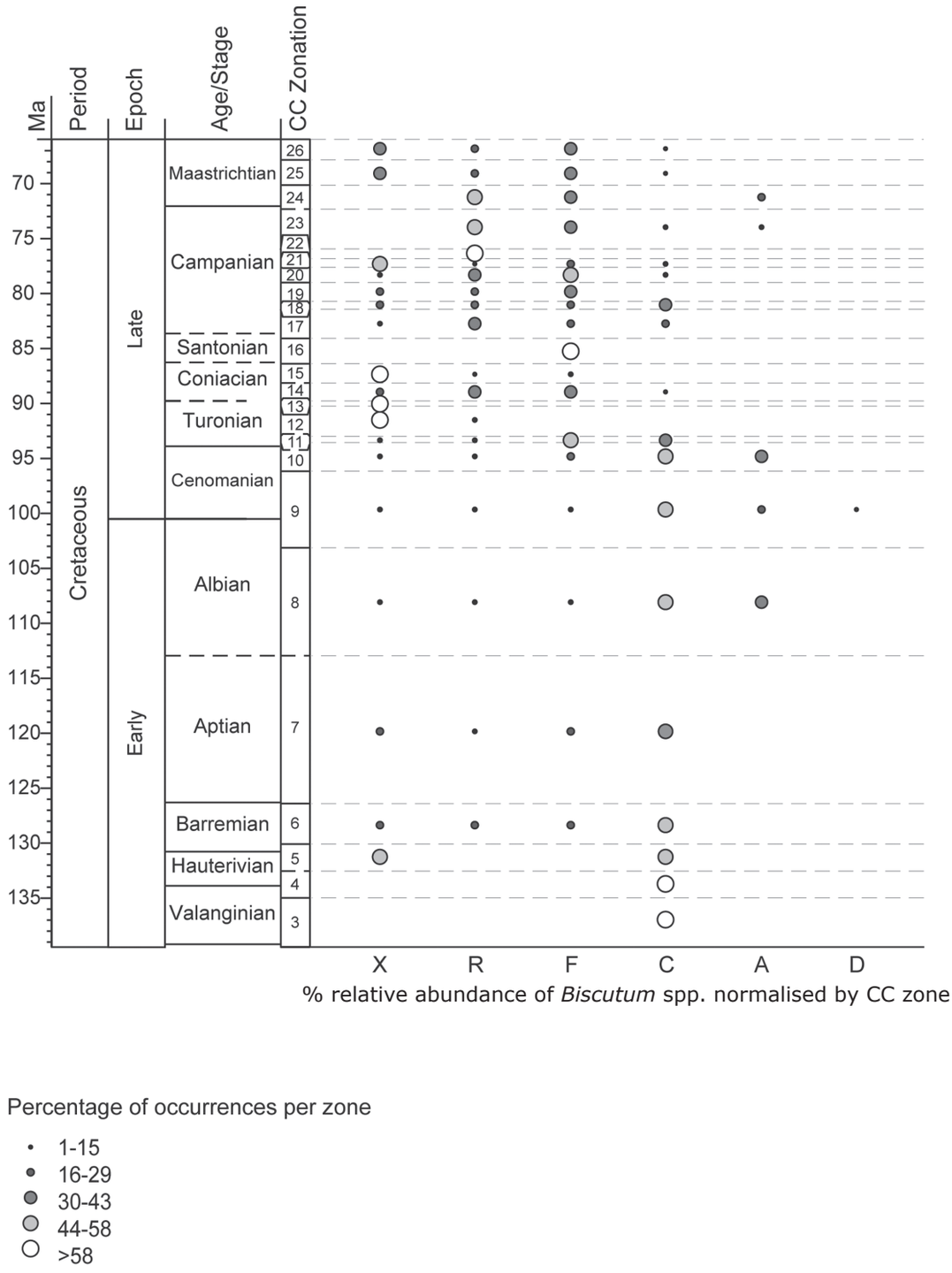

Figure 3: Semi-quantitative relative abundance of *Biscutum* plotted against time and normalised by CC zone (CC zones after Perch-Nielsen, 1985). See Table 2 for abundance categories

drologic cycle, supplying nutrients to coastal waters and potentially contributing to ocean anoxia (van Helmond *et al*., 2013).

The global impacts of OAE2 were geologically short-lived. Organic-carbon burial occurred over a discrete interval, and sea-surface temperatures gradually returned to pre-OAE2 values (*e.g*. van Helmond *et al*., 2013). The abrupt decrease in *Biscutum* abundance values, however, was not short-lived. In addition to the long-term changes in oceanographic conditions, it is also possible that the extreme palaeoceanographic conditions associated with OAE2 may have affected the role of *Biscutum* as a fertility

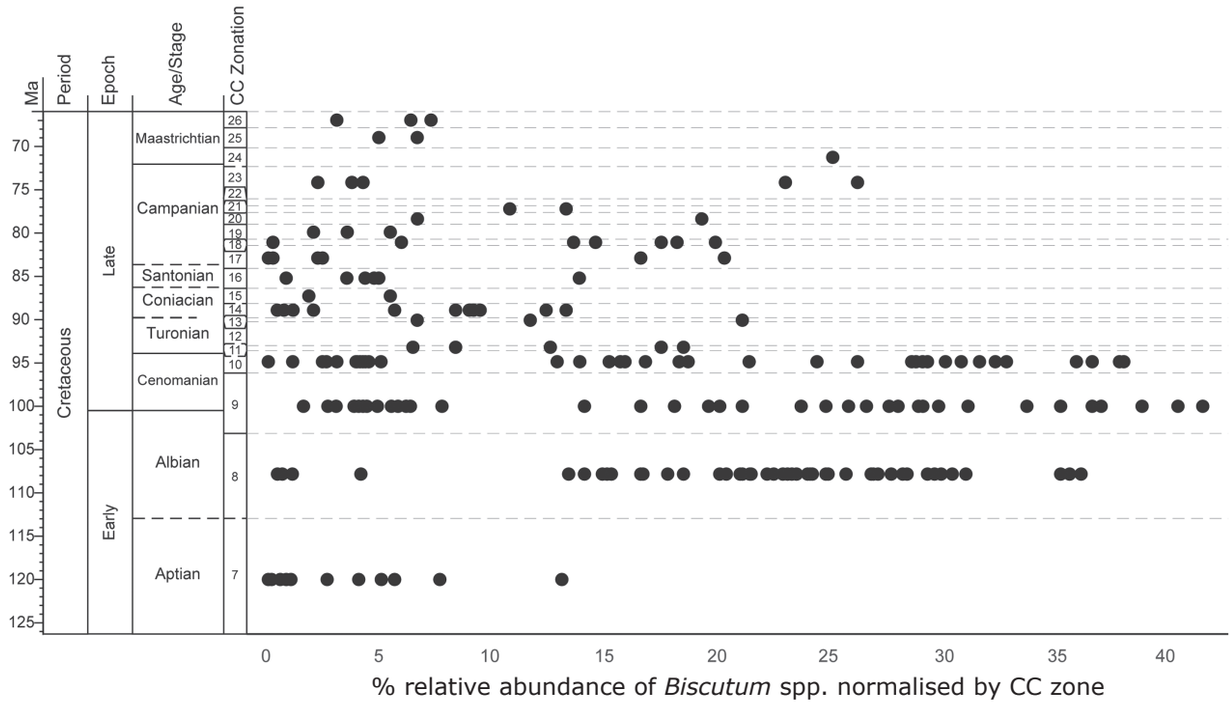

Figure 4: Quantitative relative abundance of *Biscutum* plotted against time and normalised by CC zone (CC zones after Perch-Nielsen, 1985)

indicator, as the marine plankton ecosystem was disrupted. Extreme perturbations during OAE2 may have prevented the re-establishment of *Biscutum* dominance for the rest of the Cretaceous, but it is also clear that disruption in marine plankton communities associated with OAE2 were overlain upon a pre-existing palaeoenvironmental transition, which started in the Albian at the onset of chalk deposition.

Erba (2004) investigated the decline in *Biscutum* relative abundances during OAE2. The abundance decreases documented at Eastbourne, England and Gubbio, Italy are puzzling, since many other oceanographic proxies (*e.g.* carbon isotopes) indicate that OAE2 was a time of increased, not decreased, productivity, and should contain a record of high relative abundances of fertility indicators like *Biscutum*. One hypothesis to account for the observed *Biscutum* decrease is the potential for metal toxicity, as a result of inputs from volcanism. Massive volcanism during the mid-Cretaceous likely released massive amounts of biolimiting metals into the world ocean. Increased metal levels in the oceans may have been toxic to species of coccolithophores. Erba (2004) postulated that metal toxicity may account for the differential response of the common fertility indicators *B. constans* and *Zeugrhabdotus erectus* during and after OAE2. Trace elements have been shown to play a vital role in coccolith formation (*e.g.* Okada & Honjo, 1975), although a consensus has not been reached on the exact role of each metal, likely due to species-specific responses (Jiang & Wise, 2006). Enhanced concentrations of trace metals that originated during OAE2 may have permanently altered nannofossil assemblages and prohibited the re-establishment of *Biscutum* as the primary productivity-indicator.

Two different models have been invoked to explain the widespread deposition of organic-rich black shales during OAE2: the preservational model and the productivity model. According to the preservational model, global deposition of organic-rich sediments resulted from intense stratification of the water-column due to sluggish ocean circulation. Water-column stratification prevented oxygenation at the sediment-water interface, allowing organic matter that reached the sea-floor to escape oxidation and be buried (Schlanger & Jenkyns, 1976). Conversely, the productivity model postulates generation of large amounts of organic matter as driving the deposition of organic-rich strata. Bacterial decomposition of organic matter consumes oxygen, thus resulting in a positive feedback for enhanced organic matter preservation (*e.g.* Linnert *et al.*, 2011).

Similarly, two different patterns of *Biscutum* abun-

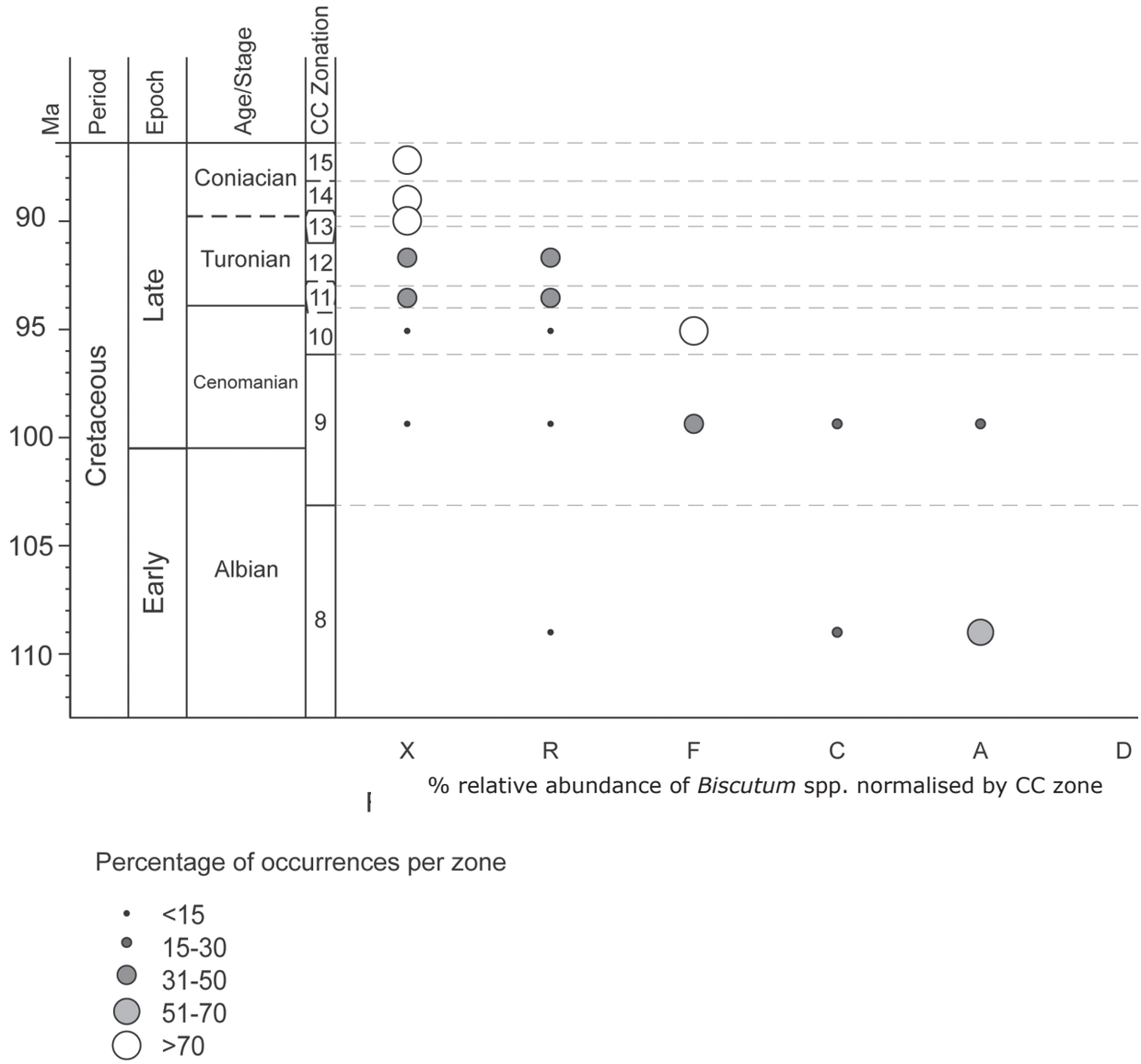

Figure 5: Quantitative relative abundance (n = 110) of *Biscutum* from low palaeolatitudes (<16˚N/S) plotted against time (CC zones after Perch-Nielsen, 1985). See Table 2 for abundance categories. Includes data from Roth (1981) and Erba (1992)

dance are observed across the Cenomanian-Turonian boundary, which have been interpreted to support either the preservational or productivity model. A decrease in abundance, or total absence, of *B. constans* has been documented in the OAE2 interval by several authors from mid-latitude sections (*e.g.* Paul *et al.*, 1999; Erba, 2004; Eleson & Bralower, 2005; Linnert *et al.*, 2010, 2011). This trend is also observed in the dataset compiled for this study (Figures 3, 4). In contrast, Hardas & Mutterlose (2007) examined sediments spanning OAE2 from Demerara Rise in the western equatorial Atlantic, and documented an increase in *Biscutum constans* throughout the OAE2 interval. Unfortunately, the paucity of zonal marker species in Hardas & Mutterlose's (2007) studied section does not allow assignment of CC zones, however, the synthesis presented in this study includes data from a broad latitudinal range (51˚S to 42˚N), including samples from palaeolatitudes similar to those examined by Hardas & Mutterlose (<15˚N/S).

Demerara Rise was located within 15˚ latitude of the Equator during the mid-Cretaceous (Suganuma & Ogg, 2006). Figure 5 presents the data subset from a palaeolatitudinal range comparable to that of Demerara Rise (<16˚N/S). Peak *Biscutum* relative abundance values through CC8 and CC9 are 'abundant', decrease to 'few' in CC10 and to 'rare' in CC11 and CC12. No occurrences were recorded from low latitudes from CC13 through

CC15. This is the same pattern that is observed in the quantitative and semiquantitative datasets containing samples with a global distribution (Figures 3, 4). The similarity in abundance patterns across broad latitudinal and oceanographic ranges suggests that the pattern of increasing abundance observed by Hardas & Mutterlose (2007) at Demerara Rise may be the result of unique and local oceanographic conditions at that site.

Additionally, results suggest that only the *B. constans*/*ellipticum*-type species experienced an abundance decrease in the mid-Cretaceous. Additional species of *Biscutum* are generally reported only at high-latitude sites, while low- to mid-latitude sites are documented as having lower species richnesses, often containing only one reported *Biscutum* species. Due to the limited number of occurrences, as well as the very low abundances reported for other species, it seems unlikely that the genus *Biscutum* maintained a consistent population while the constituent species fluctuated. The *B. constans*/*ellipticum*-type species comprise virtually all occurrences at low- to mid-latitude sites. While other species of *Biscutum* (*e.g. B. magnum, B. notaculum*) are present at high-latitude sites, they comprise only a nominal proportion of the genus.

5. Conclusions

The Cretaceous was a time of long-term oceanographic and climatic change, punctuated by severe marine perturbations in the form of OAEs, especially OAE2. *Biscutum* has been shown, in a variety of studies, to be associated with mesotrophic to eutrophic surface-water conditions. As the ocean-climate system changed dramatically through the mid-Cretaceous, black shale deposition essentially ceased, while chalk was deposited, first on continental margins, and later in the open ocean. Chalk deposition was facilitated by nutrient partitioning, stabilised ocean circulation with discrete upwelling areas, better-connected ocean basins, a stabilised thermocline and more persistent bottom-water ventilation. *Biscutum* was either ill-adapted to, or outcompeted in, new, stable oligotrophic surface-conditions, and comprised a diminishing component of nannofossil assemblages through the remainder of the Cretaceous. During OAE2, massive volcanism may have caused not only extreme high temperatures, but also may have released massive amounts of biolimiting metals into the world ocean, which may have been toxic to *Biscutum* (Erba, 2004). OAE2 may have provided enough stress to perturb the role of *Biscutum* as a fertility indicator, while the onset of nutrient partitioning and stratification prohibited the re-establishment of *Biscutum* for the remainder of the Cretaceous.

Acknowledgements

We very much appreciate the constructive reviews of Richard Howe, Joerg Mutterlose and Jamie Shamrock. The authors also thank Zachary Kita for his help in greatly improving the figures.

References

Applegate, J.L. & Bergen, J.A. 1988. Cretaceous calcareous nannofossil biostratigraphy of sediments recovered from the Galicia Margin, ODP Leg 103. *Proceedings of the ODP, Scientific Results,* **103**: 293-348.

Arthur, M.A., Dean, W.E. & Pratt, L.M. 1988. Geochemical and climatic effects of increased marine organic carbon burial at the Cenomanian/Turonian boundary. *Nature*, **335**(6192): 714-717.

Blakey, R. Late Cretaceous (85 Ma). *Paleogeography and Geologic Evolution of North America*. Retrieved October 21, 2012, from www2.nau.edu/rcb7/nam.html.

Bornemann, A., Pross, J., Reichelt, K., Herrle, J.O., Hemleben, C. & Mutterlose, J. 2005. Reconstruction of short-term palaeoceanographic changes during the formation of the Late Albian 'Niveau Breistroffer' black shales (Oceanic Anoxic Event 1d, SE France). *Journal of the Geological Society*, **162**(4): 623-639.

Bown, P.R. 2005. Selective calcareous nannofossil survivorship at the Cretaceous-Tertiary boundary. *Geology,* **33**(8): 653-656.

Bown, P.R., Lees, J.A. & Young, J.R. 2004. Calcareous nannoplankton evolution and diversity through time. *In:* H.R. Thierstein & J.R. Young (Eds). *Coccolithophores: From Molecular Processes to Global Impact*. Springer, Berlin: 481-508.

Brace, B. & Watkins, D. 2014. Evolution of the Calcareous Nannofossil Genus *Biscutum* in the middle to Upper Cretaceous North American mid-latitudes. *Micropaleontology*, **60**(4): 445-463.

Cepek, P. 1978. Mesozoic calcareous nannoplankton of the eastern North Atlantic, Leg 41. *Initial Reports of the DSDP*, **41**: 667-687.

Cepek, P. 1981. Mesozoic calcareous nannoplankton stratigraphy of the central north Pacific (mid-Pacific mountains and Hess Rise), Deep Sea Drilling Project Leg 62. *Initial Reports of the DSDP*, **62**: 397-418.

Eleson, J.W. & Bralower, T.J. 2005. Evidence of changes in surface water temperature and productivity at the Cenomanian/Turonian Boundary. *Micropaleontology*, **51**(4): 319-332.

Erba, E. 1992. Middle Cretaceous calcareous nannofossils from the western Pacific (Leg 129): evidence for paleoequatorial crossings. *Proceedings of the ODP, Scientific Results,* **129**: 189-201.

Erba, E. 2004. Calcareous nannofossils and oceanic anoxic events. *Marine Micropaleontology,* **52**: 85-106.

Erba, E. 2006. The first 150 million years history of calcareous nannoplankton: biosphere - geosphere interactions. *Palaeogeography, Palaeoclimatology, Palaeoecology*, **232**(2): 237-250.

Erba, E., Castradori, D., Guasti, G. & Ripepe, M. 1992. Calcareous nannofossils and Milankovitch cycles: The example of the Albian Gault Clay Formation (southern England). *Palaeogeography, Palaeoclimatology, Palaeoecology*, **93**: 47-69.

Forster, A., Schouten, S., Moriya, K., Wilson, P.A. & Damsté, J.S.S. 2007. Tropical warming and intermittent cooling during the Cenomanian/Turonian oceanic anoxic event 2: Sea surface temperature records from the equatorial Atlantic. *Paleoceanography*, **22**(1), PA1219.

Giorgioni, M., Weissert, H., Bernasconi, S.M., Hochuli, P.A., Keller, C.E., Coccioni, R., Petrizzo, M.R., Lukeneder, A. & Garcia, T.I. 2015. Paleoceanographic changes during the Albian-Cenomanian in the Tethys and North Atlantic and the onset of the Cretaceous chalk. *Global and Planetary Change*, **126**: 46-61.

Hardas, P. & Mutterlose, J. 2007. Calcareous nannofossil assemblages of Oceanic Anoxic Event 2 in the equatorial Atlantic: Evidence of an eutrophication event. *Marine Micropaleontology*, **66**(1): 52-69.

Hay, W. 1995. Cretaceous paleoceanography. *Geologica Carpathica*, **46**(5): 1-11.

Hay, W. 2008. Evolving ideas about the Cretaceous climate and ocean circulation. *Cretaceous Research*, **29**(5): 725-753.

van Helmond, N.A., Sluijs, A., Reichart, G.-J., Damsté, J.S.S., Slomp, C.P. & Brinkhuis, H. 2013. A perturbed hydrological cycle during Oceanic Anoxic Event 2. *Geology*, **42**(2): 123-126.

Jiang, S. & Wise, S.W., Jr. 2006. Surface-water chemistry and fertility variations in the tropical Atlantic across the Paleocene/Eocene Thermal Maximum as evidenced by calcareous nannoplankton from ODP Leg 207, Hole 1259B. *Revue de micropaléontologie*, **49**(4): 227-244.

Kulhanek, D.K. & Wise, S.W., Jr. 2006. Albian calcareous nannofossils from ODP Site 1258, Demerara Rise. *Revue de micropaléontologie*, **49**(3): 181-195.

Ladner, B.C. & Wise, S.W., Jr. 2001. Calcareous nannofossil biostratigraphy of Upper Cretaceous to Paleocene sediments from Leg 173, Iberia Abyssal Plain, Sites 1067-1069. *Proceedings of the ODP, Scientific Results,* **173**: 1-50.

Leckie, R.M., Bralower, T.J. & Cashman, R. 2002. Oceanic anoxic events and plankton evolution: Biotic response to tectonic forcing during the mid-Cretaceous. *Paleoceanography*, **17**(3): 1041.

Lees, J.A. & Bown, P.R. 2005. Upper Cretaceous calcareous nannofossil biostratigraphy, ODP Leg 198 (Shatsky Rise, northwest Pacific Ocean). *Proceedings of the ODP, Scientific Results,* **198**: 1-60.

Linnert, C., Mutterlose, J. & Erbacher, J. 2010. Calcareous nannofossils of the Cenomanian/Turonian boundary interval from the Boreal Realm (Wunstorf, northwest Germany). *Marine Micropaleontology*, **74**(1): 38-58.

Linnert, C., Mutterlose, J. & Mortimore, R. 2011. Calcareous nannofossils from Eastbourne (southeastern England) and the paleoceanography of the Cenomanian–Turonian boundary interval. *Palaios*, **26**(5): 298-313.

Moran, M.J. 1992. Biostratigraphy of Upper Cretaceous and Paleogene calcareous nannofossils from Leg 123, northeastern Indian Ocean. *Proceedings of the ODP, Scientific Results,* **123**: 381-405.

Okada, H. & Honjo, S. 1975. Distribution of coccolithophores in marginal seas along the western Pacific Ocean and in the Red Sea. *Marine Biology*, **31**(3): 271-285.

Okada, H. & Thierstein, H.R. 1979. Calcareous nannoplankton - Leg 43, Deep Sea Drilling Project. *Initial Reports of the DSDP*, **43**: 507-573.

Paul, C.R.C., Lamolda, M.A., Mitchell, S.F., Vaziri, M.R., Gorostidi, A. & Marshall, J.D. 1999. The Cenomanian–Turonian boundary at Eastbourne (Sussex, UK): a proposed European reference section. *Palaeogeography, Palaeoclimatology, Palaeoecology*, **150**(1): 83-121.

Perch-Nielsen, K. 1977. Albian to Pleistocene calcareous nannofossils from the western South Atlantic, DSDP Leg 39. *Initial Reports of the DSDP*, **39**: 699-823.

Perch-Nielsen, K. 1985. Mesozoic calcareous nannofossils. *In*: H.M. Bolli, J.B. Saunders & K. Perch-Nielsen (Eds). *Plankton Stratigraphy*. Cambridge University Press, Cambridge: 329–426.

Resiwati, P. 1991. Upper Cretaceous calcareous nannofossils from Broken Ridge and Ninetyeast Ridge, Indian Ocean. *Proceedings of the ODP, Scientific Results,* **121**: 141-170.

Roth, P.H. 1981. Mid-Cretaceous calcareous nannoplankton from the central Pacific: Implications for paleoceanography. *Initial Reports of the DSDP*, **62**: 471-489.

Roth, P.H. & Bowdler, J.L. 1981. Middle Cretaceous calcareous nannoplankton biogeography and oceanography of the Atlantic Ocean. *SEPM, Special Publication*, **32**: 517-546.

Roth, P.H. & Krumbach, K.R. 1986. Middle Cretaceous calcareous nannofossil biogeography and preservation in the Atlantic and Indian Oceans: implications for paleoceanography. *Marine Micropaleontology*, **10**(1): 235-266.

Schlanger, S.O. & Jenkyns, H.C. 1976. Cretaceous oceanic an-

oxic events: causes and consequences. *Geologie en Mijnbouw*, **55**(3-4): 179-184.

Schmidt, R.R. 1978. Calcareous nannoplankton from the western North Atlantic DSDP Leg 44. *Initial Reports of the DSDP*, **44**: 703-729.

Shamrock, J.L. & Watkins, D.K. 2009. Evolution of the Cretaceous calcareous nannofossil genus *Eiffellithus* and its biostratigraphic significance. *Cretaceous Research*, **30**(5): 1083-1102.

Stanley, S.M. & Hardie, L.A. 1998. Secular oscillations in the carbonate mineralogy of reef-building and sediment-producing organisms driven by tectonically forced shifts in seawater chemistry. *Palaeogeography, Palaeoclimatology, Palaeoecology*, **144**(1): 3-19.

Suganuma, Y. & Ogg, J.G. 2006. Campanian through Eocene magnetostratigraphy of Sites 1257–1261, ODP leg 207, Demerara rise (Western Equatorial Atlantic). *Proceedings of the ODP, Scientific Results*, **207**: 1-48.

Watkins, D.K. 1989. Nannoplankton productivity fluctuations and rhythmically-bedded pelagic carbonates of the Greenhorn Limestone (Upper Cretaceous). *Palaeogeography, Palaeoclimatology, Palaeoecology*, **74**(1): 75-86.

Watkins, D.K. & Bergen, J.A. 2003. Late Albian adaptive radiation in the calcareous nannofossil genus *Eiffellithus*. *Micropaleontology*, **49**(3): 231-251.

Watkins, D.K. & Bowdler, J.L. 1984. Cretaceous calcareous nannofossils from Deep Sea Drilling Project Leg 77, southeast Gulf of Mexico. *Initial Reports of the DSDP,* **77**: 649-674.

Watkins, D.K., Cooper, M.J. & Wilson, P.A. 2005. Calcareous nannoplankton response to late Albian oceanic anoxic event 1d in the western North Atlantic. *Paleoceanography,* **20**(2): PA2010.

Watkins, D.K., Shafik, S. & Shin, I.C. 1998. Calcareous nannofossils from the Cretaceous of the Deep Ivorian Basin, *Proceedings of the ODP, Scientific Results,* **159**: 319-333.

Watkins, D.K. & Verbeek, J.W. 1988. Calcareous nannofossil biostratigraphy from Leg 101, Northern Bahamas. *Proceedings of the ODP, Scientific Results,* **101**: 63-85.

Wiegand, G.E. 1984. Cretaceous nannofossils from the Northwest African Margin, Deep Sea Drilling Project Leg 79. *Initial Reports of the DSDP*, **79**: 563-578.

Wilson, P.A., Norris, R.D. & Cooper, M.J. 2002. Testing the Cretaceous greenhouse hypothesis using glassy foraminiferal calcite from the core of the Turonian tropics on Demerara Rise. *Geology*, **30**(7): 607-610.

Wise, S.W., Jr. 1983. Mesozoic and Cenozoic calcareous nannofossils recovered by Deep Sea Drilling Project Leg 71 in the Falkland Plateau region, southwest Atlantic Ocean. *Initial Reports of the DSDP*, **71**: 481-550.

Wise, S.W., Jr. & Wind, F.H. 1977. Mesozoic and Cenozoic calcareous nannofossils recovered by DSDP Leg 36 drilling on the Falkland Plateau, SW Atlantic sector of the Southern Ocean. *Initial Reports of the DSDP*, **36**: 296-309.